Progress In Electromagnetics Research Letters, Vol. 39, 151–159, 2013

COMPACT WIDE STOPBAND QUASI-ELLIPTIC FUNCTION LOWPASS FILTER USING QUASI-LUMPED ELEMENTS

Chen Miao, Jin Xu*, and Wen Wu

Ministerial Key Laboratory of JGMT, Nanjing University of Science and Technology, Nanjing 210094, China

Abstract—This paper presents a novel quasi-elliptic function lowpass filter (LPF) by using quasi-lumped elements. The proposed LPF is firstly based on a seven-order Chebyshev response lowpass prototype. Then, a series branches of shunt resonant LC circuit is introduced in the filter design to provide a transmission zero close to the transition band, which can improve the roll-off rate of proposed LPF significantly. To implement the lumped elements of lowpass prototype, the high-impedance meander lines are employed to realized the inductors while inter-digital microstrip lines and the microstrip parallel-plate structures are used to realize the capacitors. To validate the proposed method, a LPF with 3 dB cutoff frequency f_c at 1.9 GHz is designed and fabricated. The measured results show that the fabricated LPF has a sharp roll-off rate up to -142 dB/octave and -15 dB harmonic suppression from $1.1f_c$ to $9.7f_c$. Moreover, the fabricated LPF also has a compact size of $0.1\lambda_{gc} \times 0.11\lambda_{gc}$. Good agreement can observed between the simulation and measurement.

1. INTRODUCTION

Compact lowpass filters (LPFs) with broad stopband are in great demand for mixing products to remove undesired harmonics or spurious signals in radio frequency front-end circuits. So far, various LPF structures have been studied to implement good performance [1–12].

In [1–5], multiple same type of lowpass cells, i.e., generalized coupled-line circuit in [1], tapered compact microstrip resonant cell in [2], patch resonator in [3], double-folded spiral compact microstrip

Received 22 March 2013, Accepted 15 April 2013, Scheduled 18 April 2013

* Corresponding author: Jin Xu (xujin2njust@126.com).

resonant cell in [4] and transformed radial stub in [5], are cascaded together to construct a LPF. The used lowpass cells can be either with different sizes [1–3] or with same size [4, 5]. To further extend the stopband, parallel open-ended stub in [4] and another type of LC LPF in [5] are introduced to suppress some high-order harmonic frequencies. Since the circuit size of this type of LPF is mainly determined by its basic lowpass cell, multiple resonators used in such type of filter will result in a large circuit size [1–5]. The extra bandstop extension structure in [4, 5] will also increase the design procedure. Defected microstrip structure (DMS) and defected ground structure (DGS) are another two popular structures to develop the LPFs [6–9], mainly due to their bandgap characteristics. By properly cascading multiple DMS or DGS together, the bandstop or lowpass performance can be achieved. In [6], a very sharp skirts LPF is designed by using G-shaped DMS, but this LPF suffers from large circuit size and poor in-band return loss. By using dumbbell DGS in [7], double arrow head DGS in [8] and meander-line shaped DGS in [9], all the LPFs achieve good harmonic suppression. However, the etched ground plane in [7–9] will increase the filter installation complexity with the system. Thus, all the above reported LPFs except LPF in [6] have their limitation in the practical application. The LPFs reported in [10–12] can overcome the above problem, which achieve compact size and single plane configuration. In [10], a LPF with compact size, very simple configuration and up to the 7th harmonic suppression is reported. In [11], a radial split ring resonator loaded by folded polygon patches is applied to LPF design, and the loaded polygon patches can generate multiple transmission zeros. In [12], multiple structures with different bandstop frequency response are carefully arranged to build up a LPF with greater than the 10th harmonic suppression. The above four LPFs exhibits their own merits, but it has to admit that they also suffer from some drawbacks, i.e., poor roll-off rate in [10], 10 dB return loss in [11], and poor roll-off rate in [12].

This paper presents a novel quasi-elliptic lowpass filter (LPF) by using quasi-lumped elements. The proposed LPF structure has a transmission zero close to the transition band, resulting in a sharp roll-off rate. The lumped inductors in this paper are realized by high-impedance meander lines, and the lumped capacitors are implemented by inter-digital microstrip lines or microstrip parallel-plate structures. As an example, a LPF with 3 dB cutoff frequency at 1.9 GHz is designed and fabricated. The measured results show that the proposed LPF has the merits of good return loss, sharp roll-off rate, broad stopband and compact size. Detailed design procedure is discussed in the following sections.

2. PROPOSED QUASI-ELLIPTIC FUNCTION LPF

Figure 1(a) gives a traditional lumped-element seven-order LPF. A Chebyshev function response lowpass prototype with 0.04321 dB ripple is applied to this circuit and the lumped circuit element values of the low-pass prototype can be found to be $g = 1$, $g_1 = 1.008$, $g_2 = 1.4368$, $g_3 = 1.9398$, $g_3 = 1.622$, $g_5 = 1.9398$, $g_6 = 1.4368$, $g_7 = 1.008$ and $g_8 = 1$ [13]. When its -3 dB cutoff frequency is specified as $f_c = 1.9$ GHz, it can be calculated from the reference [13] that $C_1 = 1.844$ pF, $C_2 = 3.549$ pF, $L_1 = 6.571$ nH, $L_2 = 7.418$ nH. The line with round symbol in Figure 2 plots its typical frequency response. Although such LPF has achieved a good performance, its transition band is not sharp enough. To achieve such goal, a new C_3 is introduced to parallel with L_2, as shown in Figure 1(b). The series braches of shunt-resonant circuit L_2C_3 can generate a transmission zero and its frequency location can be given as follows:

$$f_{\mathrm{TZ}} = \frac{1}{2\pi\sqrt{L_2C_3}} \tag{1}$$

When $C_3 = 0.57$ pF and the above values of the inductors and the capacitors are employed, the line with square symbol in Figure 2 gives a typical frequency response of LPF with a transmission zero. After comparison of these two lines, a transmission zero f_z at 2.45 GHz can be observed obviously. After the TZ is introduced, f_c moves towards lower frequency and the in-band return loss becomes poor. Since the proposed quasi-elliptic function LPF given in Figure 1(b) does not belong to a classic elliptic function LPF, its lowpass prototype cannot be found directly. In this paper, the values of the inductors and the capacitors are achieved by the optimization in ADS software, so as to meet the desired electrical performance. The optimization goal for the circuit given in Figure 1(b) is specified as follows: $f_c = 1.9$ GHz, return loss better than 18 dB and $f_{\mathrm{TZ}} = 2.45$ GHz. After optimization, the values of lumped elements in Figure 1(b) are found as follows:

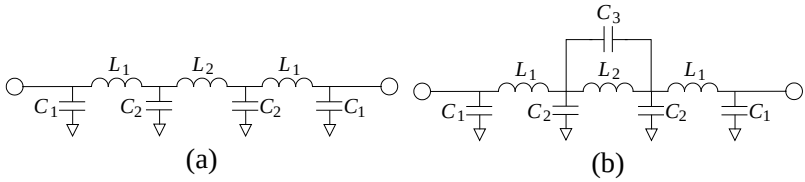

Figure 1. (a) Traditional lumped-element seven-order LPF. (b) Proposed quasi-elliptic function LPF.

$C_1 = 0.545\,\text{pF}$, $C_2 = 2.06\,\text{pF}$, $C_3 = 0.74\,\text{pF}$, $L_1 = 5.65\,\text{nH}$, $L_2 = 5.65\,\text{nH}$. Under such designing parameters, the line without symbol in Figure 2 also plots its typical frequency response. Compared such quasi-elliptic function frequency response with the Chebyshev function frequency response, it can be seen that the roll-off rate of the transition band has been improved. Although the stopband rejection becomes poor, it is still able to meet most of the application. Actually, the Chebyshev function frequency response will not achieve such higher stopband rejection, mainly due to parasitic effect, poor quality factor of the practical inductors and capacitors, etc.

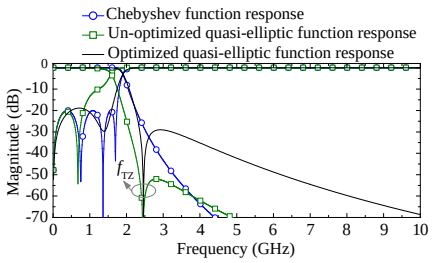

Figure 2. Typical frequency response of Chebyshev function, un-optimized and optimized quasi-elliptic function.

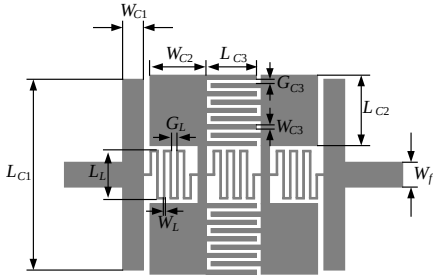

Figure 3. Physical layout of proposed quasi-elliptic function LPF.

3. LPF IMPLEMENTATION

To implement the above quasi-elliptic function response LPF at microwave frequency, the circuit shown in Figure 3 is proposed. The lumped-element inductors $L_1 \sim L_3$ are implemented by the high-impedance meander lines in Figure 3. The lumped-element capacitors C_1 and C_2 are realized by microstrip parallel-plate structures, and the lumped-element capacitor C_3 is realized by inter-digital microstrip lines. The values of $L_1 \sim L_3$ are mainly controlled by the length of the high-impedance meander lines. A longer length of the high-impedance meander lines in a larger value of inductance. The capacitance of the microstrip parallel-plate capacitor is determined by its area. A larger area of the parallel-plate results in a larger value of capacitance. The capacitance of the inter-digital microstrip line capacitor is determined by the length of the fingers, number of fingers, and the space between the fingers. A longer length of fingers, a more number of fingers and narrower space between fingers results in a larger value of capacitance.

Figure 4(a) gives the lossless equivalent lumped-element model of proposed microstrip LPF structure at low frequency [14], which considers the parasitic elements. It can be seen that the rectangular microstrip parallel-plate capacitor has the parasitic inductor $L_{C,p1}$ or $L_{C,p2}$ besides the desired $C_{p1}/2$ or $C_{p2}/2$. The high-impedance meander line inductor has the parasitic capacitor $C_{L,p1}$ besides the desired L_{p1}. The inter-digital microstrip line capacitor has the parasitic inductor $L_{C,p3}$ and the parasitic capacitor $C_{C,p3}$, besides the desired C_{p3}. Figure 4(b) gives the simplified equivalent lumped-element model of proposed microstrip LPF structure, which has a same circuit form with the circuit as shown in Figure 1(b). As shown in Figure 4(b), the parasitic inductors $L_{C,p1}$ or $L_{C,p2}$ will affect the effective capacitance of C_{r2}. It is interesting that two shunt branches of series resonant circuits $L_{C,p1}C_{p1}$ and $L_{C,p2}C_{p2}$ will produce two TZs inside the stopband, which is significant for improving stopband performance. The frequency locations of these two TZs are determined by

$$f_{\mathrm{TZ1}} = \frac{1}{\pi\sqrt{2L_{C,p1}C_{p1}}} \tag{2}$$

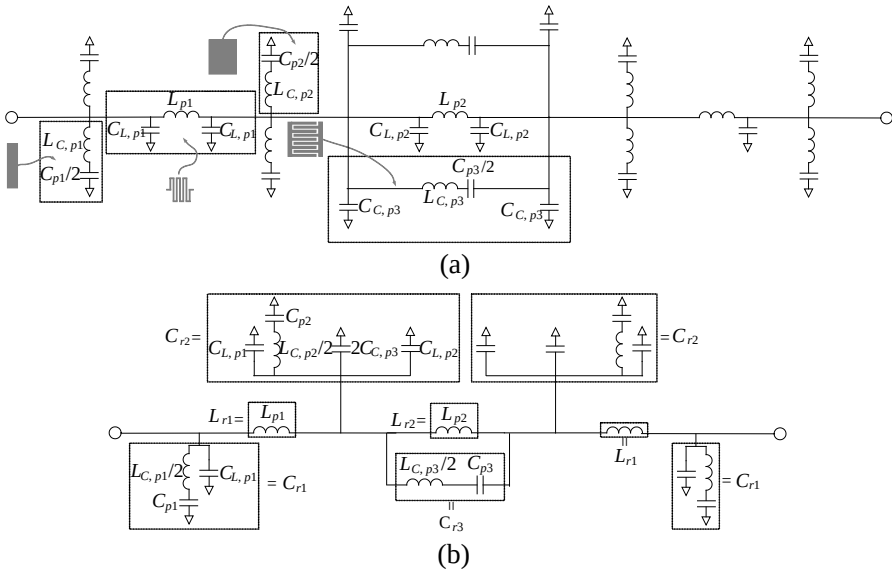

Figure 4. (a) Lossless equivalent lumped-element model of proposed LPF at low frequency. (b) Simplified equivalent lumped-element model of proposed LPF at low frequency.

$$f_{\mathrm{TZ2}} = \frac{1}{\pi\sqrt{2L_{C,p2}C_{p2}}} \tag{3}$$

The parasitic inductors $L_{C,p1}C_{p1}$ and $L_{C,p2}C_{p2}$ will also cause two spurious frequency at the stopband. Two shunt branches of hybrid circuits have bandpass performance and the frequency locations of these two spurious frequencies are given by

$$f_{sp1} = \frac{1}{2\pi}\sqrt{\frac{2(C_{p1}+C_{L,p1})}{L_{C,p1}C_{p1}C_{L,p1}}} \tag{4}$$

$$f_{sp2} = \frac{1}{2\pi}\sqrt{\frac{2\left(C_{p2}+C_{L,p1}+2C_{C,p3}+C_{L,p2}\right)}{L_{C,p2}C_{p2}\left(C_{L,p1}+2C_{C,p3}+C_{L,p3}\right)}} \tag{5}$$

The parasitic capacitor $C_{L,p1}$ will not be harmful to the circuit, which will be absorbed by the adjacent capacitors C_{r1} and C_{r2}. The series branch of series resonant circuit $L_{C,p3}C_{p3}$ will cause a spurious frequency, which is located at

$$f_{sp3} = \frac{1}{\pi\sqrt{2L_{C,p3}C_{p3}}} \tag{6}$$

In this LPF design, the value of $L_{C,p3}$ should be optimized to be as small as possible, so as to make this spurious frequency far away from the passband. After the parasitic elements are considered, the frequency location of the TZ f_{TZ} should be modified as

$$f'_{\mathrm{TZ}} = \frac{1}{\pi\sqrt{4L_{p2}C_{p3}+2L_{C,p3}C_{p3}}} \tag{7}$$

In the LPF design, the effective value of capacitance $C_{r1} \sim C_{r3}$ and inductance $L_{r1}\sim L_{r2}$ should be optimized to close to the above optimized value of quasi-elliptic function lowpass filter. The parasitic inductors $L_{C,p1}$, $L_{C,p2}$ and $L_{C,p3}$ should be optimized to be as small as possible.

4. SIMULATED AND MEASURED RESULTS

Based on the above discussion, the whole LPF structure given by Figure 3 is optimized by 3-D full-wave EM simulator HFSS, so as to consider the impact of the layout, the short connecting lines between the meandered-line inductors and parallel-plate capacitors, and some other ideality factors. The tuned physical dimensions are $W_f = 1.55\,\mathrm{mm}$, $L_{C1} = 13\,\mathrm{mm}$, $W_{C1} = 1.5\,\mathrm{mm}$, $L_{C2} = 5.1\,\mathrm{mm}$, $W_{C2} = 2.74\,\mathrm{mm}$, $L_{C3} = 2.29\,\mathrm{mm}$, $W_{C3} = 0.3$ mm, $G_{C3} = 0.3\,\mathrm{mm}$, $L_L = 2.5$, $W_L = 0.12\,\mathrm{mm}$, and $G_L = 0.2\,\mathrm{mm}$. Figure 5(a) gives the

photograph of fabricated LPF. The fabricated filter has a compact size of 11.32 mm × 13 mm, corresponding to $0.1\lambda_{gc} \times 0.11\lambda_{gc}$, where λ_{gc} represents the guided wave-length of a 50 Ω microstrip line on the used substrate at f_c.

Figure 5(b) plots the measured and the simulated S-parameters. The measured 3 dB cutoff frequency f_c is at 1.93 GHz. The IL in the passband is less than 0.4 dB, and the in-band return loss is better than 19 dB. The fabricated LPF also exhibits a sharp ROR up to −142 dB/octave. It can be seen that the upper stopband are suppressed to below 15 dB from $1.1f_c$ to $9.7f_c$. Table 1 gives a performance comparison of proposed LPF with reported works. As seen, the proposed LPF exhibits great advantages of electrical performance and circuit area.

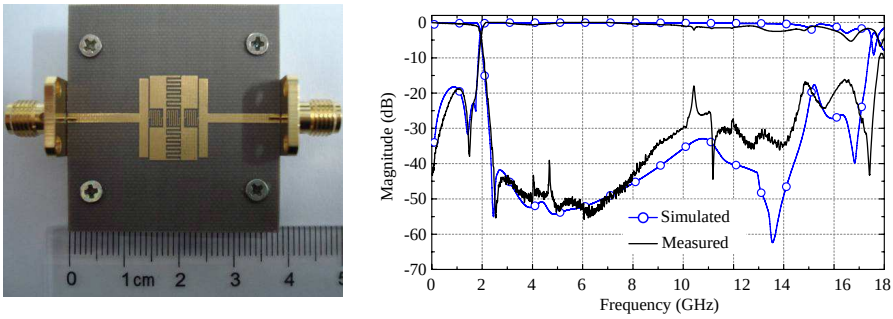

(a) (b)

Figure 5. (a) Photograph and (b) simulated and measured S-parameters of the fabricated LPF.

Table 1. Performance comparison with some reported LPFs.

	Insertion Loss (dB)	Roll-off Rate (dB/Octave)	Harmonic suppression	Circuit area (λ_g^2)
[3]	1.0	−60	$1.3f_c$~$10.5f_c$ (20 dB)	0.3 × 0.1
[5]	1.0	−144	$1.14f_c$~$13f_c$ (20 dB)	0.4 × 0.16
[10]	0.3	−76	$1.1f_c$~$8.8f_c$ (20 dB)	0.084 × 0.102
[11]	0.39	−146	$1.13f_c$–$10.8f_c$ (20 dB)	0.1 × 0.12
[12]	0.4	−39	$1.55f_c$~$16.4f_c$ (15 dB)	0.11 × 0.09
This Work	0.4	−142	$1.1f_c$~$9.7f_c$ (15 dB)	$0.1\lambda_{gc} \times 0.11\lambda_{gc}$

5. CONCLUSION

A new microstrip quasi-elliptic function lowpass filter is presented in this paper. As an example, a LPF with $f_c = 1.93\,\text{GHz}$ has been demonstrated. Results indicate that the demonstrator has the properties of compact size, good passband performance, and ultra-wide stopband. With all these good features, the proposed filter is applicable for modern communication systems.

REFERENCES

1. Wu, Y., Y. Liu, S. Li, and C. Yu, "A new wide-stopband low-pass filter with generalized coupled-line circuit and analytical theory," *Progress In Electromagetics Research*, Vol. 116, 553–567, 2011.
2. Li, L., Z.-F. Li, and Q.-F. Wei, "Compact and selective lowpass filter with very wide stopband using tapered compact microstrip resonant cells," *Elecron. Lett.*, Vol. 45, No. 5, 267–268, 2009.
3. Li, J.-L., S.-W. Qu, and Q. Xue, "Compact microstrip lowpass filter with sharp roll-off and wide stop-band," *Elecron. Lett.*, Vol. 45, No. 2, 110–111, 2009.
4. Li, K., M. Zhao, Y. Fan, Z. Zhu, and W. Cui, "Compact lowpass filter with wide stopband using novel double-folded SCMRC structure with parallel open-ended stub," *Progress In Electromagnetics Research Letters*, Vol. 36, 77–86, 2013.
5. Ka, K. and K. S. Yeo, "New ultra-wide stopband low-pass filter using transformed radial stubs," *IEEE Trans. Microw. Theory Tech.*, Vol. 59, No. 3, 604–611, 2011.
6. Cao, H., W. Guan, S. He, and L. Yang, "Compact lowpass filter with high selectivity using G-shaped defected microstrip structure," *Progress In Electromagnetics Research Letters*, Vol. 33, 55–62, 2012.
7. Chen, Q. and J. Xu, "DGS resonator with two transmission zeros and its application to lowpass filter design," *Elecron. Lett.*, Vol. 46, No. 21, 1447–1449, 2010.
8. Al Sharkawy, M. H., D. Abd El-Aziz, and E. Galal, "A miniaturized lowpass/bandpass filter using double arrow head defected ground structure with centered etched ellipse," *Progress In Electromagnetics Research Letters*, Vol. 24, 99–107, 2011.
9. Wang, C. J. and T. H. Lin, "A multi-band meandered slotted-ground-plane resonator and its application of lowpass filter," *Progress In Electromagnetics Research*, Vol. 120, 249–262, 2011.
10. Hayati, M., H. A.-D. Memari, and H. Abbasi, "Compact

microstrip lowpass filter with sharp roll-off and wide stopband using semicircle stub resonator," *Progress In Electromagnetics Research Letters*, Vol. 35, 73–81, 2012.

11. Hayati, M., H. Asadbeigi, and A. Sheikhi, "Microstrip lowpass filter with high and wide rejection band," *Elecron. Lett.*, Vol. 48, No. 19, 1217–1219, 2012.
12. Wang, J. P., H. Cui, and G. Zhang, "Design of compact microstrip lowpass filter with ultra-wide stopband," *Elecron. Lett.*, Vol. 48, No. 14, 854–856, 2012.
13. Hong, J. S. and M. J. Lancaster, *Microstrip Filter for RF/Microwave Applications*, Wiely, New York, 2001.